Cellular Physiology and Biochemistry

Cell Physiol Biochem 2018;48:158-172
DOI: 10.1159/000491715
Published online: July 12, 2018
Accepted: April 24, 2018

Original Paper

FXR Acts as a Metastasis Suppressor in Intrahepatic Cholangiocarcinoma by Inhibiting IL-6-Induced Epithelial-Mesenchymal Transition

Bei Lv[a] Lijie Ma[a] Wenqing Tang[a] Peixin Huang[a] Biwei Yang[a] Lingxiao Wang[b,c] She Chen[d] Qiang Gao[a] Si Zhang[d] Jinglin Xia[a,b]

[a]Liver Cancer Institute, Zhongshan Hospital, Fudan University, Shanghai, [b]Minhang Hospital, Fudan University, Shanghai, [c]Wenzhou Medical University, Wenzhou, [d]Key Laboratory of Glycoconjugate Research Ministry of Public Health, Department of Biochemistry and Molecular Biology, Shanghai Medical College, Fudan University, Shanghai, China

Key Words
Farnesoid X receptor • Cholangiocarcinoma • IL-6 • EMT

Abstract
Background/Aims: Intrahepatic cholangiocarcinoma (ICC) is a complicated condition, with difficult diagnosis and poor prognosis. The expression and clinical significance of the farnesoid X receptor (FXR), an endogenous receptor of bile acids, in ICC is not well understood. ***Methods:*** Western blotting and immunochemical analyses were used to determine the levels of FXR in 4 cholangiocarcinoma cell lines, a human intrahepatic biliary epithelial cell line (HIBEpic) and 322 ICC specimens, respectively, while quantitative reverse transcription polymerase chain reaction was used to detect the mRNA levels of FXR in cholangiocarcinoma cell lines. We evaluated the prognostic value of FXR expression and its association with clinical parameters. We determined the biological significance of FXR in ICC cell lines by agonist-mediated activation and lentivirus-mediated silence. IL-6 expression was tested by an enzyme-linked immunosorbent assay and flow cytometry. *In vitro*, cell proliferation was examined by Cell Counting Kit-8, migration and invasion were examined by wound healing and transwell assays; *in vivo*, tumor migration and invasion were explored in NOD-SCID mice. ***Results:*** FXR was downregulated in ICC cell lines and clinical ICC specimens. Loss of FXR was markedly correlated with aggressive tumor phenotypes and poor prognosis in patients with ICC. Moreover, FXR expression also had significant prognostic value in carbohydrate antigen 19-9 (CA19-9) negative patients. The expression of FXR was negatively correlated with IL-6 levels in clinical ICC tissues. FXR inhibited the proliferation, migration, invasion and epithelial mesenchymal transition (EMT) of ICC cells via suppression of IL-6 *in vitro*. Obeticholic acid, an agonist of FXR,

B. Lv, L. Ma and W. Tang contributed equally to this work.

Jinglin Xia
and Si Zhang

Liver Cancer Institute, Zhongshan Hospital, Fudan University
Shanghai (China)
Fax +86-21-64037318, E-Mail xia.jinglin@zs-hospital.sh.cn, zhangsi@fudan.edu.cn

inhibited IL-6 production, tumor growth and lung metastasis of ICC *in vivo*. ***Conclusions:*** FXR could be a promising ICC prognostic biomarker, especially in CA19-9 negative patients with ICC. FXR inhibits the tumor growth and metastasis of ICC via IL-6 suppression.

Introduction

Intrahepatic cholangiocarcinoma (ICC) is thought to arise from the intrahepatic biliary epithelia lining the epithelium and peribiliary glands [1]. ICC accounts for only 10–15% of all primary liver malignant cancers. However, epidemiological data have revealed a rapid increase in the incidence and mortality of ICC in recent years [2]. Unfortunately, ICC is a malignant disease with insidious onset, fast and invasive growth, a high recurrence rate and high mortality [3-5]. In a large cohort, patients with ICC suffered from postoperative recurrence and had a poor response to systemic chemotherapeutic treatments, with a five-year survival rate less than 5% [6]. The exploration of effective chemotherapies and molecularly targeted therapies is hindered by a poor understanding of ICC. Carbohydrate antigen 19-9 (CA19-9) is generally considered to be a promising predictor for ICC prognosis [7]; however, some CA19-9-negative patients with ICC show rapid disease progression. Hence, novel prognostic markers for ICC treatment are urgently needed.

Farnesoid X receptor (FXR), a ligand-activated transcription factor encoded by the *Nr1h4* gene, belongs to the nuclear receptor super family, is expressed in diverse tissues, such as the kidney, stomach, duodenum, colon, and liver. FXR is activated by bile acids (BAs) and, once activated, it could stimulate transcription of genes involved in synthesis, transport and metabolism of BAs and cholesterol [8-12]. Previously, we found that FXR protects against fructose-induced liver steatosis via inflammatory inhibition and adipose differentiation-related protein (ADRP) reduction [13]. We also found that FXR is associated with β-catenin and inhibits its activity in hepatocellular carcinoma (HCC), which indicated that FXR provides protection against hepatocarcinogenesis [14].

ICC and HCC share similar mechanism including common molecular subtypes and driver genes. Apart from its role in HCC development, evidence has begun to accumulate that FXR could be involved in ICC progression. FXR has been implicated in maintaining sterility of the biliary tract through various mechanisms, such as assisting vasoactive intestinal peptide receptor-1-induced choleresis [15], promoting the expression of α-crystalline (a molecule that prevents oxidative stress), and combining with the activated vitamin D receptor (VDR) to induce the expression of the antimicrobial peptide, cathelicidin, in biliary epithelial cells [16]. FXR also participates in the metabolism of lipids and glucose [17-20], which is related to obesity, one of the risk factors of ICC [21, 22]. However, the clinical significance and functional role of FXR in ICC still remains elusive.

In the present study, we aimed to investigate the expression and clinical significance of FXR in ICC. We found that FXR was significantly downregulated in ICC and loss of FXR correlated with poor prognosis of patients with ICC. In addition, FXR acted as a powerful marker of prognosis in CA19-9 negative patients. FXR expression was negatively correlated with the IL-6 level in patients with ICC. FXR activation inhibited ICC growth and metastasis via IL-6 suppresssion *in vitro* and *in vivo*.

Materials and Methods

Human ICC Samples

Human liver tumor tissues were obtained from surgically resected specimens from patients with ICC at Zhongshan Hospital, Fudan University (Shanghai, P.R. China). Archived paraffin-embedded tumor tissues collected from 322 patients with ICC treated between 2005 and 2011 were used for tissue microarray construction and immunohistochemistry. Overall survival (OS) and time to recurrence (TTR) were defined as a time frame from the date of surgery to death and recurrence, respectively. If recurrence had not

appeared or patients were still alive at the last follow-up, data was censored. Fresh tumor samples from 97 ICC patients were collected for the IL-6 tests.

All patients were diagnosed with ICC according to the World Health Organization criteria [23]. The Edmondson grading system was used to define tumor differentiation [24]. Liver function was assessed using the Child–Pugh scoring system. The seventh edition of the tumor-node-metastasis (TNM) classification system was used [25]. Follow-up data was collected until June 2016. The median following up was 25 months (range, 4–126 months).

Antibodies and reagents

The FXR antibody for immunohistochemistry (IHC) and western blotting was bought from Abcam (Cambridge, UK). Anti-SHP, E-cadherin, N-cadherin, Snail, β-catenin, Vimentin, ZO-1, β-actin, and α-tubulin antibodies were purchased from Cell Signaling Technology (CST, Boston, USA). Polybrene and mitomycin C were bought from Sigma-Aldrich (St. Louis, MO, USA). The FXR agonist, obeticholic acid (OCA) was purchased from Selleck Chemicals (Houston, TX, USA). Recombinant IL-6 was obtained from R&D Systems (Minneapolis, USA), and the anti-IL-6 monoclonal antibody was purchased from Abcam (Cambridge, UK).

Immunohistochemistry and evaluation system

Tissue microarrays (TMAs) were deparaffinized with xylene, rehydrated in serially diluted alcohol, and subsequently processed in a microwave for 15 min with Tris-EDTA (pH = 6.0) buffer for antigen retrieval. After blocking of endogenous peroxidase with 3% H_2O_2, the sections were immersed in 3% bovine serum albumin diluted with phosphate-buffered saline (PBS) for 60 min. The slides were then incubated with anti-FXR antibodies (1:100 dilution) for 60 min at 37 °C. After rinsing three times with PBS, the tissue sections were incubated with HRP-conjugated streptavidin for 15 min at room temperature. Slides were then washed with PBS three times, counterstained with hematoxylin and eosin, dehydrated, and mounted for histological examination [26].

All sections were viewed and scored by two pathologists, using the double blind method. The final results were the mean of the scores for ICC TMAs and their copies by the two pathologists. According to the scores, the lowest was 0 and the highest was 6. The definition of the calculated scores was as follows: 0 point, negative staining; 1~2 points weak staining (+); 3–4 points, moderate staining (++); and 5–6 points, strong staining (+++). We classified the FXR immunostaining score as low expression when the final score was 0–2 and high expression when the final score was 3–6 [27].

Cell lines and treatment

The human intrahepatic biliary epithelial cell line (HIBEpic), and the human cholangiocarcinoma cell lines RBE, HCCC-9810, HuCCT1, and CCLP1 were purchased from Chinese Academy of Sciences Shanghai Branch Cell Bank (Shanghai, China). Cell lines were cultured in Roswell Park Memorial Institute (RPMI) Medium 1640 (Gibco, GrandIsland, NY, USA) supplemented with 10% fetal calf serum (FBS; Gibco, GrandIsland, NY, USA), 1% penicillin and streptomycin (Gibco, GrandIsland, NY, USA) at 37 °C with 5% CO_2.

Recombinant human IL-6 was used to pretreat RBE and CCLP1 cells. The cells were cultured in the presence of exogenous IL-6 (20 ng/mL). The amount of anti-IL-6 antibody added into the medium according to the manufacturer's statement that 20 pg of the antibody neutralizes 1U of IL-6 activity. IL-6 and its antibody were added into the culture medium at the beginning of the assay. FXR activation was established in culture medium with 1 μM OCA for 24 hours [14].In order to exclude the effect of proliferation, we used mitomicin C (10 μg/ml for 2 hours) to pretreat the cells in woung healing essay.

Infection and stable clone selection

Lentiviral vectors containing FXR shRNA, Plko.1-puro empty control vector and RFP were purchased from the Gene company (Shanghai, China) [13]. The plasmids were packaged into VSV-G pseudotyped letiviral particles after transfected into 293T cells with the pACKH1 packaging plasmid mix (System Biosciences, Mountain View, California, USA) according to the manufacturer's instructions. The indicated cell lines were separately infected with these different viral supernatants containing 4 μg/mL of polybrene. The cells were selected by puromycin (1.5 μg/mL) and validated by western blotting.

Enzyme-linked immunosorbent assay (ELISA)

Tumor tissues from all patients with ICC were washed three times in cooled physiological saline to remove the blood and then dried with filter paper, weighed, 0.5 g was homogenized with 5 mL of physiological saline. After centrifugation, the supernatant was retained. IL-6 levels in the supernatants were detected using an ELISA kit according to the manufacturer's instructions (R&D, Minneapolis, USA). The cell supernatants of the ICC lines were centrifuged before testing.

Flow cytometry

The expression level of IL-6 was detected by flow cytometry according to the manufacturer's instructions (BD Biosciences, San Jose, CA, USA). Data was acquired with Diva (BD Biosciences, San Jose, CA, USA) and analyzed using FlowJo software (TreeStar).

Quantitative reverse transcription polymerase chain reaction (qRT-PCR) and western blotting

qRT-PCR was performed to assess mRNA expression on an ABI Prism 7500 Sequence Detection system according to the manufacturer's protocol. FXR forward primer: 5'-TCCGGACATTCAACCATCAC-3', reverse primer: 5'-TCACTGCACATCCCAGATCTC-3'. β-actin forward primer: 5'-GCACCACACCTTCTACAATG-3', reverse primer: 5'- TGCTTGCTGATCCACATCTG -3'. Total protein lysates extracted from cells and in order to explore the translocate of β-catenin, nuclear protein was extracted using a nuclear protein extraction kit (Pierce, USA). The protein was quantitated using a BCA Protein Assay Kit (Pierce, USA), then subjected to sodium dodecyl sulfate-polyacrylamide gel electrophoresis (SDS-PAGE), transferred onto polyvinylidene difluoride membranes, and incubated with the corresponding antibodies. The experiments were repeated independently three times.

Cell functional experiments

A Cell Counting Kit-8 (Dojindo, shanghai, China) was used to detect the cell proliferation ability according to the manufacturer's specifications, as previous described [24]. Wound healing assays were performed as previously described [29], all the cells were cultured with 1% FBS in RPMI 1640 culture media. The width of the wound was measured under the microscope at 0 h and 48 h after wounding to estimate the migratory ability of the ICC cells. Then we repeated the wound healing essay using mitomycin C (10μg/mL for 2 hours) to block the proliferation of ICC cells. The effect of FXR and IL-6 on cell invasion and migration were assessed using transwell assays, as described previously [28]. Each assay was repeated at least three times.

In vivo assays for tumor growth and metastasis

RBE cells were chosen for tumor implantation because of its highly tumorigenicity *in vivo* [29, 30] compared with HuCCT1 and CCLP1. To make it easier to track the lung metastatic nodes, we used RBE-RFP cells. Cells (5×10^6) were suspended in 100 μL of serum-free RPMI 1640 and Matrigel (BD Biosciences, San Jose, CA, USA; 1:1) and injected subcutaneously into the upper left flank region of NOD-SCID mice. The mice were observed over 5 weeks for tumor formation. The tumor volume was measured twice weekly using a caliper and calculated as follows: $V\ (cm^3) = ab^2/2$ [a and b represented the largest and smallest tumor diameters measured at necropsy]. One week after inoculation, we fed one group of NOD-SCID mice with 10 mg/kg/day OCA; the control group was fed with vehicle solution. Upon sacrifice, the tumors were recovered and the volume of each tumor was determined. Part of the tumor tissue was taken for IL-6 testing. The lungs were removed and embedded in paraffin, and the total number of lung metastases was counted under the microscope, as described previously [31].

Statistical analyses

Statistical analyses were carried out using SPSS software 20.0 (IBM SPSS, New York, NY, USA). The chi-square test was used to analyze the categorical data. The Kaplan–Meier method was performed to estimate the survival rate and the Cox proportional hazards regression model for multivariate survival analysis was used to evaluate the predictable value of recurrence and the survival rate. Correlation analysis was used to test the correlation between IL-6 and FXR. Student's *t* test was used to analyze comparisons between groups. A P value of < 0.05 (two-tailed) was considered statistically significant, and a P value of < 0.01 (two-tailed) was considered very significant.

Results

FXR is downregulated in ICC and correlates with tumor size and metastasis

We performed IHC analysis to determine the expression and location of FXR in tumor tissues and matched non-tumor liver tissues from 332 patients with ICC. FXR positive signals were mainly localized in the nucleus (Fig. 1a). The staining intensity of FXR in tumors was much lower than that in intrahepatic small bile duct cells, which have almost the same expression level of FXR as hepatocytes (Fig. 1a–c). IHC staining using TMAs of 322 patients with ICC indicated that FXR expression was scored as negative or weak in most tumor tissues (176 of 322: negative, n=122; weak, n=54), while moderate or strong in most corresponding non-tumor liver tissues (222 of 322: moderate, n=103; strong, n=119) (Fig. 1c).

Loss of FXR correlates with aggressive clinicopathological characteristics in patients with ICC

We further investigated the correlation between FXR expression and the clinicopathological features of patients with ICC. Based on the IHC results, all 322 patients with ICC were dichotomized as FXR^{low} (n = 176) and FXR^{high} (n = 146). Clinicopathologic analysis showed that loss of FXR was significantly correlated with tumor size ($P < 0.001$), lymph node metastasis ($P = 0.007$), vascular invasion ($P = 0.016$), tumor number ($P = 0.036$), tumor differentiation ($P = 0.003$), and TNM stage ($P < 0.001$) (Table 1).

Loss of FXR correlates with poor prognosis in ICC patients

We further investigated the prognositic value of FXR in this cohort of 322 patients. Kaplan–Meier curves analysis showed that patients in the FXR^{low} group had significantly shorter TTR (time to recurrence) (median TTR 34.54 and 60.48 months, respectively; difference = 25.94 months; $P < 0.001$) and worse OS (overall survival) (median OS 35.84 and 67.41 months, respectively; difference = 31.57 months; $P < 0.001$) (Fig. 1d) compared with those in the FXR^{high} group. Univariate analysis also indicated that loss of FXR was associated with worse TTR (hazard ratio [HR] = 0.508, 95% CI 0.380–0.679, $P < 0.001$) and poor OS (HR = 0.503, 95% CI 0.376–0.672, $P < 0.001$) (Table 2 and Table 3). Therefore, FXR expression in the tumor tissue could be considered as a relatively independent factor in the predicting prognosis of ICC patients.

FXR has prognostic value in CA19-9-negative patients with ICC

Several clinical studies demonstrated that the preoperative serum CA19-9 level is a promising predictor for ICC prognosis [7, 32, 33]. A low CA19-9 level is generally associated with favorable prognosis. Nevertheless, some

Table 1. FXR expression and clinicopathological parameters. Abbreviations: HCC, hepatocellular carcinoma; HBsAg, hepatitis B surface antigen, HCVAb, hepatitis C virus antibody; TNM, tumor-nodes-metastases; Bold p-values less than 0.05 indicate statistical significance

Variables		N	FXR low	FXR high	P
Age (years)					
	≤ 58	169	93	76	0.911
	< 58	153	83	70	
Gender					
	Male	128	67	61	0.568
	Female	194	109	85	
HBsAg					
	Negative	199	108	91	0.908
	Positive	123	68	55	
HCVAb					
	Negative	319	174	145	1.000
	Positive	3	2	1	
Size(cm)					
	≤ 5	145	61	84	0.000
	> 5	177	115	62	
Number					
	Single	244	125	119	0.036
	Multiple	78	51	27	
Lymphatic invasion					
	Absent	266	136	130	0.007
	Present	56	40	16	
Vascular invasion					
	Absent	276	143	133	0.016
	Present	46	33	13	
Tumor encapsulation					
	Absent	39	18	21	0.304
	Present	283	158	125	
Differentiation					
I–II		187	89	98	0.003
	III–IV	135	87	48	
CA199 (U/mL)					
	≥ 37	163	84	79	0.265
	>37	159	92	67	
Cirrhosis					
	No	236	126	110	0.527
	Yes	86	50	36	
TNM stage					
I +II		247	121	126	0.000
III+IV		75	55	20	

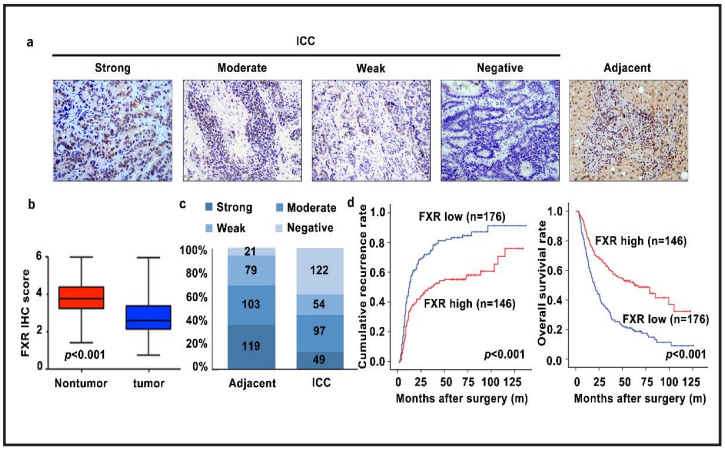

Fig. 1. Downregulation of FXR was associated with poor prognosis in patients with ICC. a Representative immunostaining images of FXR in ICC and paired adjacent non-tumor tissues. b The expression of FXR in paired tumor and non-tumor tissues are compared by IHC scoring. c Scores of immunochemistry staining of FXR in 322 cases. d Kaplan–Meier analysis of time to recurrence rate (TTR) and overall survival (OS) for FXR expression.

patients with negative CA19-9 developed rapidly. Unfortunately, there is no reliable biomarker to differentiate the prognosis of CA19-9-negative patients. We hence tested the prognostic value of FXR in CA19-9-negative patients (cut-off point 37 U/mL). Among the 322 patients with ICC, 50.06% (163/322) patients had a negative CA19-9 serum level (< 37 U/mL). In these CA19-9-negative patients, we found that patients with negative FXR had an obviously worse TTR (TTR: 37.00 ± 5.20 months, $P < 0.001$) and OS (OS: 43.91 ± 4.43 months, $P < 0.001$) compared with patients with positive FXR (TTR: 66.48 ± 6.24 months, OS: 75.56 ± 5.74 months) (Fig. 2a) In CA19-9-positive patients, we found that patients whose CA19-9 > 200 ng/mL had significantly worse prognosis, including shorter TTR ($P<0.001$) and OS ($P<0.001$), than patients whose CA19-9 < 200 ng/mL (Fig. 2b), which was consistent with previous report [34].

Table 2. Univariate and Multivariate Analyses of Factors Associated with Time to Recurrence in 322 iCCA Patients. Abbreviations: TNM, tumor–node–metastasis; CI, confidence interval; Bold p-values less than 0.05 indicate statistical significance

Variables	Univariate		Multiviariate	
	HR (95 % CI)	P value	HR (95 % CI)	P value
Gender (female vs male)	1.086(0.817-1.443)	0.572		
Age (years) (≤ 58 vs. > 58)	0.876(0.662-1.158)	0.353		
Tumor size (diameter, cm) (≤ 5 vs. > 5)	1.443(1.088-1.914)	0.011	1.306(0.984-1.734)	0.065
Tumor number (multiple vs. single)	1.728(1.264-2.360)	0.001	1.492(1.092-2.039)	0.012
Tumor thrombus (absent vs. present)	1.349(0.897-2.030)	0.151		
Tumor encapsulation (absent vs. present)	1.450(0.922-2.283)	0.108		
Tumor differentiation (I/II vs. III/IV)	1.573(1.186-2.086)	0.002	1.471 (1.044-2.074)	0.028
Cirrhosis (yes vs. no)	1.218(0.893-1.662)	0.214		
Lymph node metastasis	2.364(1.678-3.30)	0.000	2.025(1.128-3.633)	0.018
CA19-9	1.296(0.981-1.712)	0.068		
TNM stage	2.008(1.470-2.742)	0.000	0.806(0.445-1.458)	0.475
Hepatitis history	0.883(0.663-1.176)	0.395		
FXR	0.521(0.391-0.695)	0.000	0.508(0.380-0.679)	0.000

Table 3. Univariate and Multivariate Analyses of Factors Associated with Overall Survival in 322 iCCA Patients. Abbreviations: TNM, tumor–node–metastasis; CI, confidence interval; Bold p-values less than 0.05 indicate statistical significance

Variables	Univariable		Multivariable	
	HR (95 % CI)	P value	HR (95 % CI)	P value
Gender (female vs. male)	1.142(0.870-1.499)	0.339		
Age (years) (≤ 58 vs. > 58)	1.006(0.772-1.311)	0.965		
Tumor size (diameter, cm) (≤ 5 vs. > 5)	1.529(1.168-2.003)	0.002	1.239(0.933-1.646)	0.139
Tumor number (multiple vs. single)	1.576(1.168-2.127)	0.003	1.401(1.032-1.901)	0.031
Tumor thrombus (absent vs. present)	1.254(0.870-1.808)	0.225		
Tumor encapsulation (absent vs. present)	1.384(0.905-2.118)	0.134		
Tumor differentiation (I/II vs. III/IV)	2.014(1.540-2.635)	0.000	1.509(1.069-2.132)	0.019
Cirrhosis (yes vs. no)	0.994(0.709-1.395)	0.973		
Lymph node metastasis	2.716(1.969-3.747)	0.000	2.050(1.144-3.672)	0.016
CA19-9	1.631(1.250-2.126)	0.000	1.541(1.177-2.017)	0.002
TNM stage	2.245(1.675-3.010)	0.000	0.750(0.413-1.360)	0.343
Hepatitis history	0.803 (0.611-1.056)	0.116		
FXR	0.432(0.326-0.569)	0.000	0.503(0.376-0.672)	0.000

FXR inhibits IL-6 production in ICC cell lines

We detected the expression of FXR by western blotting and qPCR in four ICC cell lines, as well as a normal biliary epithelial cell line HIBEpic. Loss of FXR was observed in most ICC cell lines except RBE cells (Fig. 3a and b). Previous studies have shown that IL-6 is a critical pathogenic factor for ICC [35]. Thus, we explored whether FXR could regulate the expression of IL-6 in ICC cell lines. HuCCT1, which has a relative low level of endogenous FXR, was stimulated with the FXR agonist OCA, whose treatment for patients with primary cholestasis has entered clinical trials [36]. RBE and CCLP1 cells, with a relatively high level of endogenous FXR, were infected with FXR-shRNA lentivirus. FXR activation and knockdown efficiencies were confirmed using western blotting (Fig. 3a–d). The results showed

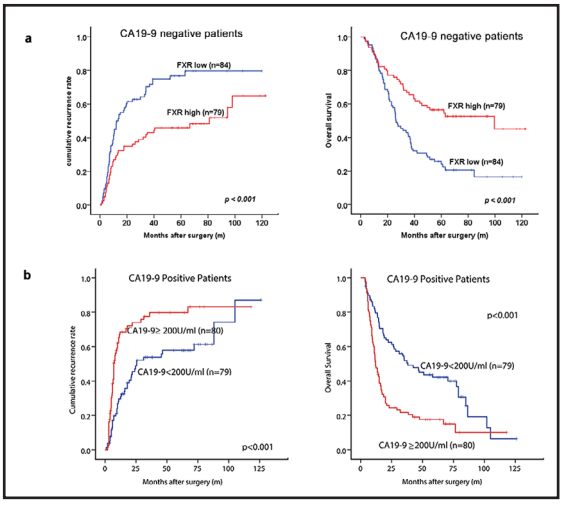

Fig. 2. The prognostic value of CA19-9 and FXR in ICC Patients. a Kaplan–Meier curves for TTR (left panel)and OS (right panel) of ICC patients with negative CA19-9 (CA19-9 < 37 U/mL) based on FXR expression in ICC (n=163). b Kaplan–Meier curves for TTR (left panel) and OS (right panel) of ICC patients with positive CA19-9 (CA19-9 ≥ 37 U/mL) based on CA19-9 expression in ICC (n=159).

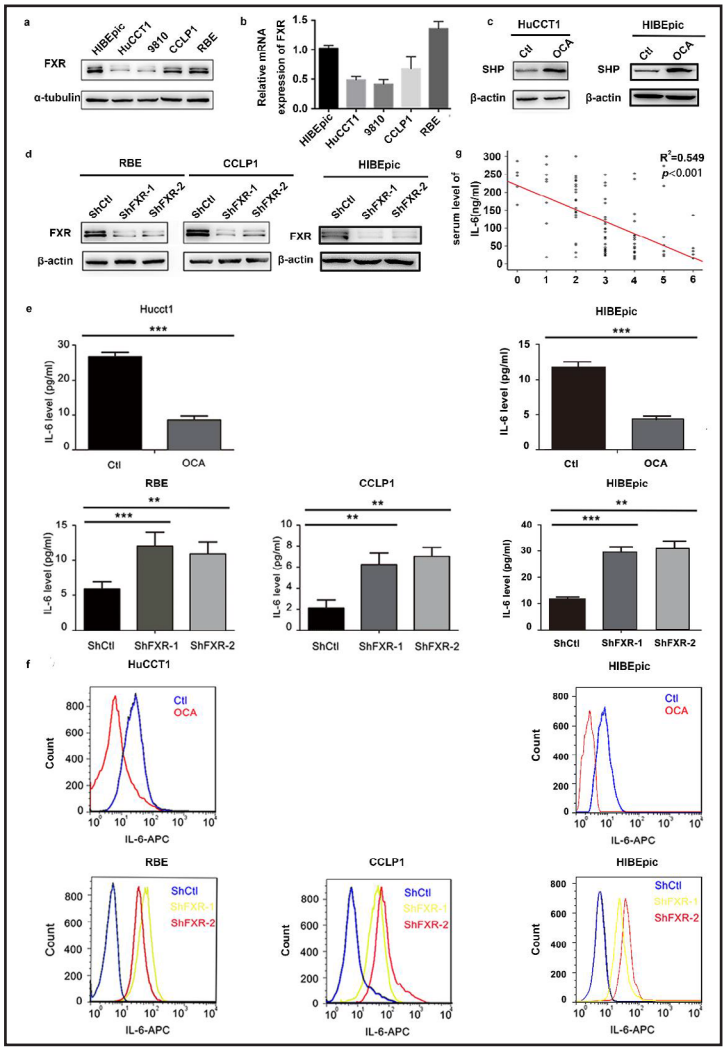

Fig. 3. The inhibitory effect of FXR on IL-6 production in ICC cell lines and the negative correlation between FXR and IL-6 in patients with ICC. a Expression of FXR in an immortalized human intrahepatic biliary epithelial cell line (HIBEpic) and four cholangiocarcinoma cell lines. α-tubulin was used as the control. b Relative FXR mRNA level in an immortalized human intrahepatic biliary epithelial cell line (HIBEpic) and four cholangiocarcinoma cell lines. β-actin was used as the control. c HuCCT1 cells (left panel) and HIBEpic cells (right panel) were activated with the FXR agonist OCA (1 μM), and control solvent. d CCLP1, RBE and HIBEpic cells were infected with lentiviral FXR shRNAs (shFXR-1 and shFXR-2) and lentiviral shCtl vector. Efficiency of activation and knockdown of FXR was verified by western blotting. e IL-6 level in the culture supernatant of FXR-activated ICC cells and healthy HIBEpic cells was detected by ELISA (upper panel). IL-6 level in the culture supernatant of FXR-silenced ICC cells and healthy HIBEpic cells was detected by ELISA (lower panel). f IL-6 level in FXR-activated ICC cells and healthy HIBEpic cells was detected by flow cytometry (upper panel). IL-6 level in FXR-silenced ICC cells and healthy HIBEpic cells was detected by flow cytometry (lower panel). g Correlation analysis between FXR expression (IHC score) and IL-6 level (ELISA) in 97 patients with ICC.

that IL-6 decreased when FXR was activated in HuCCT1 cells, while it increased when FXR was knocked down in CCLP1 and RBE cells (Fig. 3e and f). We also got the similar result in normal biliary epithelial cells HIBEpic (Fig.3c, d, e and f).

Loss of FXR correlates with increased IL-6 levels in patients with ICC

Among the autocrine cytokines generated in the inflammatory tumor microenvironment of HCC and ICC, IL-6 seems to be pivotal in the initiation and development of experimental HCC and ICC because of its contribution to advanced hepatocellular/biliary damage and proliferation of malignant cells [37-39]. To test the effect of FXR on IL-6 *in vivo*, we detected the IL-6 level in the tumor tissue of 97 patients with ICC randomly selected from 2015 February to 2016 August. We found that FXR expression was negatively correlated with the tumor IL-6 levels in the 97 patients ($R^2 = 0.549$, $P < 0.001$) (Fig. 3g).

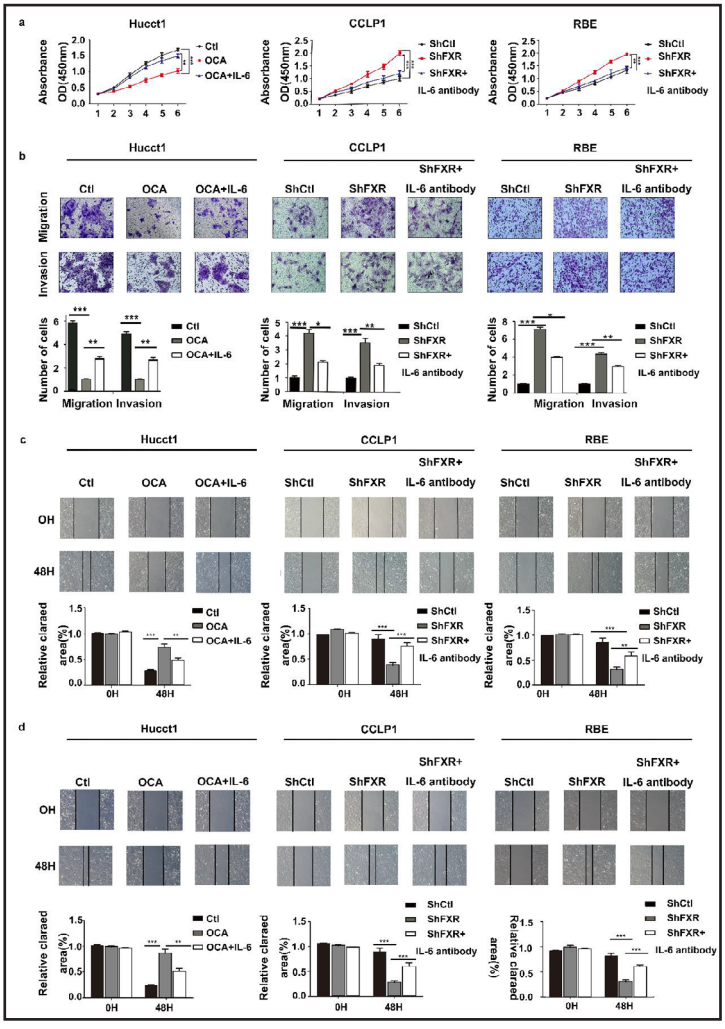

Fig. 4. The inhibitory effect of FXR on the proliferation, migration and invasion of ICC cells. a HuCCT1 cells (left panel) were treated with OCA (1 μM) and control solvent in the presence and absence of IL-6 (20 ng/mL). CCLP1 cells (middle panel) and RBE cells (right panel) were infected with lentiviral FXR shRNAs (shFXR) vectors and lentiviral control vector in the presence and absence of IL-6 antibody. Cell growth curves were measured by CCK8 test. b The effect of FXR activation and knockdown on the cell migration (left panel) and invasion (middle panel) was examined by transwell chamber assay. Representative images are shown. Magnification: ×200. All results indicate mean ± SD in triplicate using bar graph (right panel). c The effect of FXR activation and knockdown on cell migration was also confirmed by scratch wound healing assay (upper panel). Representative images are shown. Magnification: ×200. All results indicate the mean ± SD for triplicate experiments using a bar graph (lower panel). **P<0.01, ***P<0.001. d The inhibitory effect of FXR on migration of ICC cells was independent of proliferation suppression. HuCCT1 cells (left panel) were treated with OCA (1 μM) and control solvent in the presence and absence of IL-6 (20 ng/mL). CCLP1 cells (middle panel) and RBE cells (right panel) were infected with lentiviral FXR shRNAs (shFXR) and lentiviral control vector (shCtl) in the presence and absence of IL-6 antibody. The effect of FXR activation and knockdown on cell migration was examined by scratch wound healing assay. Cells were pretreated with mitomycin C (10 μg/ml for 2 h) before the assays. Representative images are shown (upper panel). Magnification: ×200. All results indicate the mean ± SD for triplicate experiments using a bar graph (lower panel). **P<0.01, ***P<0.001.

FXR inhibits proliferation, migration, and invasion of ICC cells via IL-6 suppression

The clinical implications of FXR in ICC prompted us to explore its potential biological function. We first compared the proliferative ability in FXR-activated and FXR-silenced cells with their respective controls. The proliferation of FXR-activated HuCCT1 cells was significantly inhibited, while the proliferation of CCLP1-shFXR and RBE-shFXR cells was markedly enhanced, compared with their respective controls (Fig. 4a). FXR-activated HuCCT1 cells showed decreased cell migration and invasion compared with control cells, as measured by transwell and wound healing assays (Fig. 4b and c). In contrast, FXR-silenced cells showed increased cell migration and invasion compared with control cells (Fig. 4b and c). However, when we added IL-6 into the culture medium, the inhibitory effect of the FXR agonist OCA was rescued. Similarly, when IL-6 antibodies were added into the culture medium, the promotive effect of FXR-silencing was diminished in CCLP1 and RBE cells (Fig. 4. b and c). In order to exclude the effect of proliferation on wound healing assay, we repeated this assay using mitomicin C (10 μg/mL for 2 hours) and obtained the similar results (Fig. 4d). Taken together, FXR could inhibit the proliferation, migration, and invasion abilities of ICC cells, while IL-6 could rescue these effects *in vitro*.

FXR inhibits epithelial-mesenchymal transition (EMT) via IL-6 suppression

EMT is one of the most critical processes that provide cancer cells with increased migratory and invasive abilities [40]. Therefore, key molecules of EMT were evaluated in both FXR-activated and silenced ICC cells. Western blotting analysis indicated decreased epithelial markers, such as E-cadherin and ZO-1, and increased mesenchymal markers, such as N-cadherin, snail and Vimentin in FXR activated HuCCT1 cells compared with controls (Fig. 5a). Conversely, increased E-cadherin and ZO-1, and decreased N-cadherin, snail and Vimentin were observed in FXR-silenced CCLP1 and RBE cells (Fig. 5b). The nuclear accumulation of β-catenin, which translocates to the nucleus after EMT activation, was inhibited in FXR-activated ICC cells and promoted in FXR-silenced ICC cells (Fig. 5c and d). In accordance with functional assays, IL-6 and IL-6 antibodies could rescue the inhibitory effect of FXR activation and promotive effect of FXR silencing on EMT, respectively (Fig. 5a-d). Taken together, our results suggested that the FXR agonist OCA might inhibit EMT via IL-6 suppression in ICC cells.

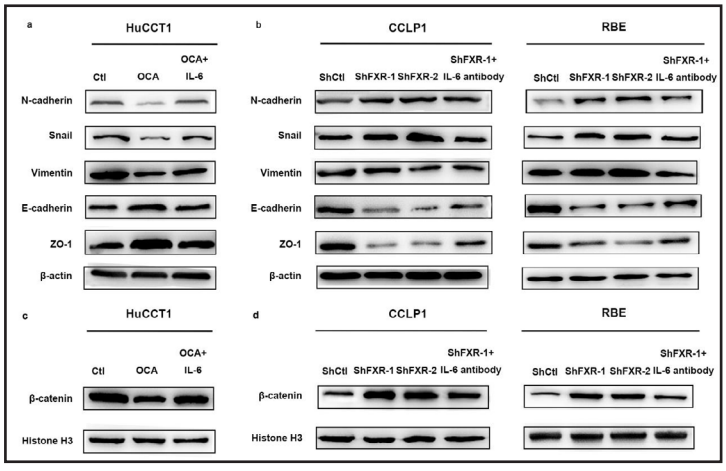

Fig. 5. The inhibitory effect of FXR on EMT of ICC cells. a HuCCT1 cells were treated with OCA (1 μM) and control solvent in the presence and absence of IL-6 (20 ng/mL). EMT-related proteins were examined by western blotting. β-actin was used as a control. b CCLP1 cells (left panel) and RBE cells (right panel) were infected with lentiviral shFXR-1, shFXR-2 and lentiviral shCtl vector in the presence and absence of IL-6 antibody. EMT-related proteins were examined by western blotting. β-actin was used as a control. c HuCCT1 cells were treated as indicated in Fig. 5a. The nuclear β-catenin level was examined by western blotting. Histone H3 was used as a control. d CCLP1 cells (left panel) and RBE cells (right panel) were treated as indicated in Fig. 5b. The nuclear β-catenin level was examined by western blotting. Histone H3 was used as a control.

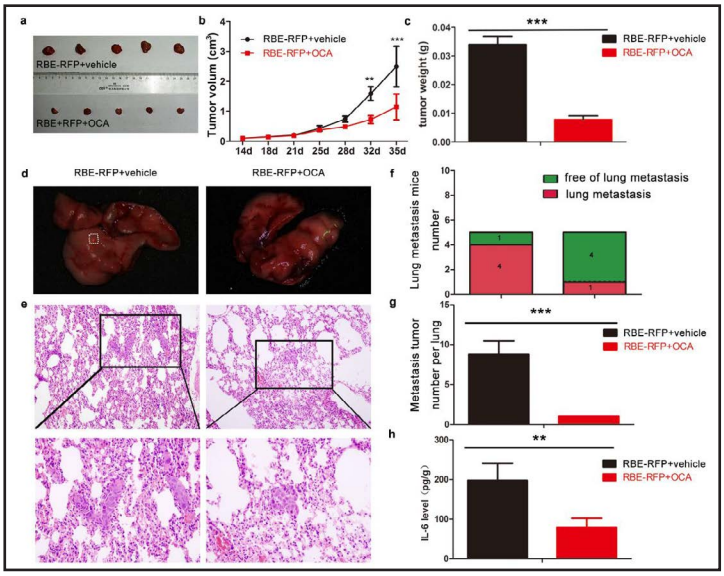

Fig. 6. OCA inhibited the growth and lung metastasis of ICC cells in vivo. RBE-RFP cells were injected subcutaneously into NOD-SCID mice. One week after inoculation, tumor bearing mice were fed with OCA (10 mg/kg/day) and vehicle solution. a Representative images of harvested tumors of the two group; b The growth curve of subcutaneous tumors in NOD-SCID mice is shown. c. Total tumor weight of the two groups. d The red fluorescence indicating lung metastasis. e Hematoxylin and eosin staining of lung metastatic nodes of NOD-SCID mouse in the control group (left panels) and the lung of the OCA group (right panels). Upper panels: magnification: ×100; bottom panels: magnification: ×200. f The number of NOD-SCID mice which had lung metastasis of the two groups, **P<0.01, ***P<0.001. g The number of lung metastasis in NOD-SCID mice of the two groups, **P<0.01, ***P<0.001. h IL-6 level in tumor tissue of NOD-SCID mice of the two groups.

FXR inhibits ICC growth and metastasis in tumor xenograft models

We evaluated whether FXR plays a crucial role in the progression of ICC in a NOD-SCID mouse tumor xenograft model. RBE-RFP cells successfully formed tumors after orthotropic transplantation into NOD-SCID mice. The tumor size of the RBE-RFP cells-derived xenografts was 2.50 ± 0.63 cm^3, which was significantly larger than that of tumors formed in NOD-SCID mice that were fed with OCA (1.15 ± 0.63 cm^3; $P < 0.01$) (Fig. 6a and b). Similarly, the tumor weight of RBE-RFP cells-derived xenografts was 34 ± 2.8 mg, which was significantly larger than that of tumors formed in NOD-SCID mice fed with OCA (7.8 ± 1.30 mg; $P < 0.001$) (Fig. 6a and c). Pulmonary metastasis occurred in 80% (4/5) of the RBE-RFP-derived xenografts, which was a higher rate than that observed in the NOD-SCID mice fed with OCA (20%, 1/5) (Fig. 6d, e and f). The number of metastatic nodules of each grade in the lung was also greater in the control RBE-RFP group (Fig. 6d, e and g). These results suggested that OCA, an FXR agonist, could inhibit tumor growth and lung metastasis in tumor xenograft models.

We next investigated the tumor tissue IL-6 level from NOD-SCID mice. Mice that were fed with OCA had a much lower IL-6 level compared with the control group (197.84 ± 43.15 pg/g *vs.* 78.95 ± 23.19 pg/g, $P < 0.01$) (Fig. 6h).

Discussion

ICC, a highly fatal tumor, is the most frequent primary malignant liver tumor next to HCC. The prognosis of ICC remains extremely poor because of the special anatomical location and physiological activity of ICC. Compared with HCC, little is known about the molecular mechanism of the pathogenesis of ICC. New prognostic indices for ICC are urgently needed because of the limitation of CA199 in ICC patients. In the present study, we demonstrated the prognostic value of FXR expression in ICC. Importantly, we showed that FXR had prognostic value in CA19-9 negative patients with ICC. Moreover, loss of FXR changed the IL-6 level in patients with ICC.

FXR plays a vital role in maintaining the balance of BAs metabolism in the liver. In the normal physiological state, once BAs increase, FXR is strongly activated, promoting the excretion of BAs and reducing their reabsorption; thus, the concentration of BAs is reduced in

the bile duct, which avoids excessive BAs damage to the liver bile duct cells. In patients with ICC, the secretion and reabsorption of BAs are switched into an aberrant state because of abnormal tumor metabolism. A large number of BAs accumulate in the bile ducts in patients with ICC, while according to our results, FXR expression decreased in the bile ducts. These effects led to excessive toxic BAs accumulation, along with damage to bile duct epithelial cells. The consequent inflammatory response could result in malignant transformation and stimulation of cholangiocarcinoma growth [41].

Increasing evidence had demonstrated a close relationship between FXR and cholangiocarcinoma. Mice deficient for FXR spontaneously developed hepatobiliary malignancies [42, 43]. Martinez-Becerra et al [44]. and Dai et al [27]. previously showed downregulation of FXR mRNA and protein in ICC patients, respectively. However, the sample size was quite limited (12 patients with ICC in Martinez-Becerra's research and 26 patients with ICC in Dai's research). Our results complemented and reinforced the above conclusion, added new finding in this field. We demonstrated a significant loss of FXR in ICC tissues and a close correlation of reduced FXR expression in tumor tissues with increased IL-6 level, poor survival and high recurrence rates in patients with ICC. These results emphasized the potential prognostic value of FXR in ICC.

Compared with HCC, patients with ICC have a relative worse prognosis. Generally, CA19-9-negative patients with ICC have a relatively favorable prognosis. However, some CA19-9-negative patients with ICC progress rapidly, with poor prognosis. To date, a satisfactory prognostic factor for CA19-9-negative patients with ICC has not been discovered. In the present study, when applied to preoperative serum CA19-9-negative patients, FXR positive status could effectively differentiate patients with poor prognosis. Thus, to some extent, FXR expression could be a powerful tool to make rational treatment decisions in CA19-9 negative patients.

A recent study demonstrated that IL-6 has an integral role in ICC prognosis as a growth and survival factor of cholangiocarcinoma cells [45]. IL-6 and its receptor cannot be detected in the serum of healthy people, but can be detected in 100% of patients with bile duct cancer, in 92.9% of those with HCC, in 53.8% of those with liver metastatic colorectal cancer, and in 40% of those with benign biliary tract disease [31]. In the present study, we observed that FXR expression was negatively correlated with tumor IL-6 levels in patients with ICC. In line with our results, Xu et al [46]. reported that FXR activation could attenuate liver inflammatory damage by suppressing inflammation mediators such as IL-6 in an animal model of lipopolysaccharide-induced liver injury. Vavassori et al [47]. reported that FXR activation decreased the severity of inflammation by reducing proinflammatory cytokines, including IL-6, in animal models of colitis. Yang et al [48]. reported that FXR-deficient mice could spontaneously develop hepatobiliary malignancies with increased IL-6 levels. Maran et al [49]. reported that FXR deficiency promoted IL-6-mediated inflammation and tumorigenesis in chemical carcinogen-induced mice intestinal cancer. These important observations in animal models, combined with our findings on human subjects, implied that FXR regulates autocrine-paracrine communication among ICC cells by IL-6 inhibition. Previous studies revealed that NF-κB activated IL-6 transcription through a consensus NF-κB binding site [50]. While FXR has been reported to antagonize NF-κB in hepatic inflammatory response [51]. We hence proposed that FXR might suppress the expression of IL-6 by NF-κB inhibition. However, the detailed mechanism still need further investigation.

EMT, which refers to the pathway of the transformation of epithelial cells to mesenchymal cells, plays a critical role in embryonic development, chronic inflammation, tissue remodeling, cancer metastasis, and a variety of fibrotic diseases. Previous reports showed that IL-6 could induce EMT in breast cancer, pancreatic cancer, and lung cancer [52-54]. In the present study, we verified that IL-6 is an autocrine factor that promotes EMT of ICC cells. At the same time, its expression was inhibited by OCA, which is an FXR agonist used for the oral treatment of cholestatic liver diseases, including primary billiary cirrhosis, non-alcoholic fatty liver disease, and non-alcoholic steatohepatitis [55, 56]. These results suggested that OCA might be a useful tool for treating patients with ICC.

Conclusion

In summary, this study indicated that loss of FXR plays a pivotal role in tumorigenesis of ICC patients and acted as a prognostic marker, especially in CA19-9-negative patients with ICC. The FXR agonist OCA might represent a novel drug to treat ICC.

Abbreviations

ICC (Intrahepatic cholangiocarcinoma); FXR (the farnesoid X receptor); CA19-9 (carbohydrate antigen 19-9); EMT (epithelial mesenchymal transition); BAs (bile acids); ADRP (adipose differentiation-related protein); HCC (hepatocellular carcinoma); VDR (vitamin D receptor); OS (Overall survival); TTR (time to recurrence); TNM (tumor-node-metastasis); IHC (immunohistochemistry); TMAs (Tissue microarrays); PBS (phosphate-buffered saline); OCA (obeticholic acid); HIBEpic (human intrahepatic biliary epithelial cell line); RPMI (Roswell Park Memorial Institute); ELISA (Enzyme-linked immunosorbent assay); qRT-PCR (quantitative reverse transcription polymerase chain reaction); SDS-PAGE (sodium dodecyl sulfate-polyacrylamide gel electrophoresis); HR (hazard ratio).

Acknowledgements

This work was supported by the National Natural Science Foundation of China [grant numbers 81572395, 81573423, 81371268, 81770137 81772615], the Shanghai Leading Academic Discipline Project [grant number B115], and the Foundation of Shanghai Outstanding Academic Leaders [grant number 14XD1401100].

Ethical approval for human subjects was obtained from the Research Ethics Committee of Zhongshan Hospital, and informed consent was obtained from each patient. The protocols for animal care and experimentation were conducted in strict accordance with the guidelines established by the Shanghai Medical Experimental Animal Care Commission. Ethical approval was obtained from the Zhongshan Hospital Research Ethics Committee.

Disclosure Statement

No potential conflict of interests exist.

References

1 Shin HR, Oh JK, Masuyer E, Curado MP, Bouvard V, Fang YY, Wiangnon S, Sripa B, Hong ST: Epidemiology of cholangiocarcinoma: an update focusing on risk factors. Cancer Sci 2010;101:579-585.
2 Khan SA, Taylor-Robinson SD, Toledano MB, Beck A, Elliott P, Thomas HC: Changing international trends in mortality rates for liver, biliary and pancreatic tumours. J Hepatol 2002;37:806-813.
3 Singh P, Patel T: Advances in the diagnosis, evaluation and management of cholangiocarcinoma. Curr Opin Gastroenterol 2006;22:294-299.
4 Valle J, Wasan H, Palmer DH, Cunningham D, Anthoney A, Maraveyas A, Madhusudan S, Iveson T, Hughes S, Pereira SP, Roughton M, Bridgewater J: Cisplatin plus gemcitabine versus gemcitabine for biliary tract cancer. N Engl J Med 2010;362:1273-1281.
5 Tan JC, Coburn NG, Baxter NN, Kiss A, Law CH: Surgical management of intrahepatic cholangiocarcinoma--a population-based study. Ann Surg Oncol 2008;15:600-608.
6 FARLEY DR, WEAVER AL, NAGORNEY DM: Natural-history of unresected cholangiocarcinoma - patient outcome after noncurative intervention. Mayo Clin Proc 1995;70:425-429.
7 Qin XL, Wang ZR, Shi JS, Lu M, Wang L, He QR: Utility of serum ca19-9 in diagnosis of cholangiocarcinoma: in comparison with cea. World J Gastroenterol 2004;10:427-432.

8 Stedman C, Liddle C, Coulter S, Sonoda J, Alvarez JG, Evans RM, Downes M: Benefit of farnesoid x receptor inhibition in obstru ctive cholestasis. Proc Natl Acad Sci U S A 2006;103:11323-11328.
9 Sinal CJ, Tohkin M, Miyata M, Ward JM, Lambert G, Gonzalez FJ: Targeted disruption of the nuclear receptor fxr/bar impairs bile acid and lipid homeostasis. Cell 2000;102:731-744.
10 Prawitt J, Abdelkarim M, Stroeve JH, Popescu I, Duez H, Velagapudi VR, Dumont J, Bouchaert E, van Dijk TH, Lucas A, Dorchies E, Daoudi M, Lestavel S, Gonzalez FJ, Oresic M, Cariou B, Kuipers F, Caron S, Staels B: Farnesoid x receptor deficiency improves glucose homeostasis in mouse models of obesity. Diabetes 2011;60:1861-1871.
11 Zhang Y, Lee FY, Barrera G, Lee H, Vales C, Gonzalez FJ, Willson TM, Edwards PA: Activation of the nuclear receptor fxr improves hyperglycemia and hyperlipidemia in diabetic mice. Proc Natl Acad Sci U S A 2006;103:1006-1011.
12 Watanabe M, Horai Y, Houten SM, Morimoto K, Sugizaki T, Arita E, Mataki C, Sato H, Tanigawara Y, Schoonjans K, Itoh H, Auwerx J: Lowering bile acid pool size with a synthetic farnesoid x receptor (fxr) agonist induces obesity and diabetes through reduced energy expenditure. J Biol Chem 2011;286:26913-26920.
13 Liu X, Xue R, Ji L, Zhang X, Wu J, Gu J, Zhou M, Chen S: Activation of farnesoid x receptor (fxr) protects against fructose-induced liver steatosis via inflammatory inhibition and adrp reduction. Biochem Biophys Res Commun 2014;450:117-123.
14 Liu X, Zhang X, Ji L, Gu J, Zhou M, Chen S: Farnesoid x receptor associates with beta-catenin and inhibits its activity in hepatocellular carcinoma. Oncotarget 2015;6:4226-4238.
15 Chignard N, Mergey M, Barbu V, Finzi L, Tiret E, Paul A, Housset C: Vpac1 expression is regulated by fxr agonists in the human gallbladder epithelium. Hepatology 2005;42:549-557.
16 D'Aldebert E, Biyeyeme BMM, Mergey M, Wendum D, Firrincieli D, Coilly A, Fouassier L, Corpechot C, Poupon R, Housset C, Chignard N: Bile salts control the antimicrobial peptide cathelicidin through nuclear receptors in the human biliary epithelium. Gastroenterology 2009;136:1435-1443.
17 Zhang Y, Lee FY, Barrera G, Lee H, Vales C, Gonzalez FJ, Willson TM, Edwards PA: Activation of the nuclear receptor fxr improves hyperglycemia and hyperlipidemia in diabetic mice. Proc Natl Acad Sci U S A 2006;103:1006-1011.
18 Lambert G, Amar MJ, Guo G, Brewer HJ, Gonzalez FJ, Sinal CJ: The farnesoid x-receptor is an essential regulator of cholesterol homeostasis. J Biol Chem 2003;278:2563-2570.
19 Ma K, Saha PK, Chan L, Moore DD: Farnesoid x receptor is essential for normal glucose homeostasis. J Clin Invest 2006;116:1102-1109.
20 Xu J, Li Y, Chen WD, Xu Y, Yin L, Ge X, Jadhav K, Adorini L, Zhang Y: Hepatic carboxylesterase 1 is essential for both normal and farnesoid x receptor-controlled lipid homeostasis. Hepatology 2014;59:1761-1771.
21 Chaiteerakij R, Yang JD, Harmsen WS, Slettedahl SW, Mettler TA, Fredericksen ZS, Kim WR, Gores GJ, Roberts RO, Olson JE, Therneau TM, Roberts LR: Risk factors for intrahepatic cholangiocarcinoma: association between metformin use and reduced cancer risk. Hepatology 2013;57:648-655.
22 Kinoshita M, Kubo S, Tanaka S, Takemura S, Nishioka T, Hamano G, Ito T, Tanaka S, Ohsawa M, Shibata T: The association between non-alcoholic steatohepatitis and intrahepatic cholangiocarcinoma: a hospital based case-control study. J Surg Oncol 2016
23 Pe'Er JJ, Stefanyszyn M, Hidayat AA: Nonepithelial tumors of the lacrimal sac. Am J Ophthalmol 1994;118:650-658.
24 Wittekind C: [pitfalls in the classification of liver tumors]. Pathologe 2006;27:289-293.
25 Edge SB, Compton CC: The american joint committee on cancer: the 7th edition of the ajcc cancer staging manual and the future of tnm. Ann Surg Oncol 2010;17:1471-1474.
26 Lv B, Zhao H, Bai X, Huang S, Fan Z, Lu J, Tang R, Yin K, Gao P, Liu B, Cheng J: Entecavir promotes cd34(+) stem cell proliferation in the peripheral blood and liver of chronic hepatitis b and liver cirrhosis patients. Discov Med 2014;18:227-236.
27 Dai J, Wang H, Shi Y, Dong Y, Zhang Y, Wang J: Impact of bile acids on the growth of human cholangiocarcinoma via fxr. J Hematol Oncol 2011;4:41.
28 Gu FM, Li QL, Gao Q, Jiang JH, Zhu K, Huang XY, Pan JF, Yan J, Hu JH, Wang Z, Dai Z, Fan J, Zhou J: Il-17 induces akt-dependent il-6/jak2/stat3 activation and tumor progression in hepatocellular carcinoma. Mol Cancer 2011;10:150.

29 Wang P, Lv L: Mir-26a induced the suppression of tumor growth of cholangiocarcinoma via krt19 approach. Oncotarget 2016;7:81367-81376.
30 Ma L, Dong P, Liu L, Gao Q, Duan M, Zhang S, Chen S, Xue R, Wang X: Overexpression of protein o-fucosyltransferase 1 accelerates hepatocellular carcinoma progression via the notch signaling pathway. Biochem Biophys Res Commun 2016;473:503-510.
31 Zhou SL, Dai Z, Zhou ZJ, Chen Q, Wang Z, Xiao YS, Hu ZQ, Huang XY, Yang GH, Shi YH, Qiu SJ, Fan J, Zhou J: Cxcl5 contributes to tumor metastasis and recurrence of intrahepatic cholangiocarcinoma by recruiting infiltrative intratumoral neutrophils. Carcinogenesis 2014;35:597-605.
32 Miwa S, Miyagawa S, Kobayashi A, Akahane Y, Nakata T, Mihara M, Kusama K, Soeda J, Ogawa S: Predictive factors for intrahepatic cholangiocarcinoma recurrence in the liver following surgery. J Gastroenterol 2006;41:893-900.
33 Abdel Wahab M, Fathy O, Elghwalby N, Sultan A, Elebidy E, Abdalla T, Elshobary M, Mostafa M, Foad A, Kandeel T, Abdel Raouf A, Salah T, Abu Zeid M, Abu Elenein A, Gad Elhak N, ElFiky A, Ezzat F: Resectability and prognostic factors after resection of hilar cholangiocarcinoma. Hepato-gastroenterology 2006;53:5-10.
34 Kondo N, Murakami Y, Uemura K, Sudo T, Hashimoto Y, Sasaki H, Sueda T: Elevated perioperative serum ca 19-9 levels are independent predictors of poor survival in patients with resectable cholangiocarcinoma. J Surg Oncol 2014;110:422-429.
35 Mott JL, Gores GJ: Targeting il-6 in cholangiocarcinoma therapy. AM J Gastroenterol 2007;102:2171-2172.
36 Fiorucci S, Cipriani S, Mencarelli A, Baldelli F, Bifulco G, Zampella A: Farnesoid x receptor agonist for the treatment of liver and metabolic disorders: focus on 6-ethyl-cdca. Mini Rev Med Chem 2011;11:753-762.
37 Prieto J: Inflammation, hcc and sex: il-6 in the centre of the triangle. J Hepatol 2008;48:380-381.
38 Park J, Tadlock L, Gores GJ, Patel T: Inhibition of interleukin 6-mediated mitogen-activated protein kinase activation attenuates growth of a cholangiocarcinoma cell line. Hepatology 1999;30:1128-1133.
39 Cheon YK, Cho YD, Moon JH, Jang JY, Kim YS, Kim YS, Lee MS, Lee JS, Shim CS: Diagnostic utility of interleukin-6 (il-6) for primary bile duct cancer and changes in serum il-6 levels following photodynamic therapy. Am J Gastroenterol 2007;102:2164-2170.
40 Lamouille S, Xu J, Derynck R: Molecular mechanisms of epithelial-mesenchymal transition. Nat Rev Mol Cell Biol 2014;15:178-196.
41 Lozano E, Sanchez-Vicente L, Monte MJ, Herraez E, Briz O, Banales JM, Marin JJ, Macias RI: Cocarcinogenic effects of intrahepatic bile acid accumulation in cholangiocarcinoma development. Mol Cancer Res 2014;12:91-100.
42 Kim I, Morimura K, Shah Y, Yang Q, Ward JM, Gonzalez FJ: Spontaneous hepatocarcinogenesis in farnesoid x receptor-null mice. Carcinogenesis 2007;28:940-946.
43 Yang F, Huang X, Yi T, Yen Y, Moore DD, Huang W: Spontaneous development of liver tumors in the absence of the bile acid receptor farnesoid x receptor. Cancer Res 2007;67:863-867.
44 Martinez-Becerra P, Vaquero J, Romero MR, Lozano E, Anadon C, Macias RI, Serrano MA, Grane-Boladeras N, Munoz-Bellvis L, Alvarez L, Sangro B, Pastor-Anglada M, Marin JJ: No correlation between the expression of fxr and genes involved in multidrug resistance phenotype of primary liver tumors. Mol Pharm 2012;9:1693-1704.
45 Isomoto H, Mott JL, Kobayashi S, Werneburg NW, Bronk SF, Haan S, Gores GJ: Sustained il-6/stat-3 signaling in cholangiocarcinoma cells due to socs-3 epigenetic silencing. Gastroenterology 2007;132:384-396.
46 Xu Z, Huang G, Gong W, Zhou P, Zhao Y, Zhang Y, Zeng Y, Gao M, Pan Z, He F: Fxr ligands protect against hepatocellular inflammation via socs3 induction. Cell Signal 2012;24:1658-1664.
47 Vavassori P, Mencarelli A, Renga B, Distrutti E, Fiorucci S: The bile acid receptor fxr is a modulator of intestinal innate immunity. J Immunol 2009;183:6251-6261.
48 Yang F, Huang X, Yi T, Yen Y, Moore DD, Huang W: Spontaneous development of liver tumors in the absence of the bile acid receptor farnesoid x receptor. Cancer Res 2007;67:863-867.
49 Maran RR, Thomas A, Roth M, Sheng Z, Esterly N, Pinson D, Gao X, Zhang Y, Ganapathy V, Gonzalez FJ, Guo GL: Farnesoid x receptor deficiency in mice leads to increased intestinal epithelial cell proliferation and tumor development. J Pharmacol Exp Ther 2009;328:469-477.
50 Libermann TA, Baltimore D: Activation of interleukin-6 gene expression through the nf-kappa b transcription factor. Mol Cell Biol 1990;10:2327-2334.

51 Wang YD, Chen WD, Wang M, Yu D, Forman BM, Huang W: Farnesoid x receptor antagonizes nuclear factor kappab in hepatic inflammatory response. Hepatology 2008;48:1632-1643.
52 Sullivan NJ, Sasser AK, Axel AE, Vesuna F, Raman V, Ramirez N, Oberyszyn TM, Hall BM: Interleukin-6 induces an epithelial-mesenchymal transition phenotype in human breast cancer cells. Oncogene 2009;28:2940-2947.
53 Huang C, Yang G, Jiang T, Zhu G, Li H, Qiu Z: The effects and mechanisms of blockage of stat3 signaling pathway on il-6 inducing emt in human pancreatic cancer cells *in vitro*. Neoplasma 2011;58:396-405.
54 Dehai C, Bo P, Qiang T, Lihua S, Fang L, Shi J, Jingyan C, Yan Y, Guangbin W, Zhenjun Y: Enhanced invasion of lung adenocarcinoma cells after co-culture with thp-1-derived macrophages via the induction of emt by il-6 Immunol Lett 2014;160:1-10.
55 Sepe V, Bifulco G, Renga B, D'Amore C, Fiorucci S, Zampella A: Discovery of sulfated sterols from marine invertebrates as a new class of marine natural antagonists of farnesoid-x-receptor. J Med Chem 2011;54:1314-1320.
56 De Marino S, Ummarino R, D'Auria MV, Chini MG, Bifulco G, Renga B, D'Amore C, Fiorucci S, Debitus C, Zampella A: Theonellasterols and conicasterols from theonella swinhoei. Novel marine natural ligands for human nuclear receptors. J Med Chem 2011;54:3065-3075.